Orientation of phenylphosphonic acid self-assembled monolayers on a transparent conductive oxide: A combined NEXAFS, PM-IRRAS, and DFT study

ARTICLE *in* LANGMUIR · FEBRUARY 2013

Impact Factor: 4.46 · DOI: 10.1021/la304594t · Source: PubMed

Langmuir

Article

pubs.acs.org/Langmuir

Orientation of Phenylphosphonic Acid Self-Assembled Monolayers on a Transparent Conductive Oxide: A Combined NEXAFS, PM-IRRAS, and DFT Study

Matthew Gliboff,[†] Lingzi Sang,[‡] Kristina M. Knesting,[§] Matthew C. Schalnat,[‡] Anoma Mudalige,[‡] Erin L. Ratcliff,[‡] Hong Li,[∥] Ajaya K. Sigdel,[⊥,#] Anthony J. Giordano,[∥] Joseph J. Berry,[#] Dennis Nordlund,[¶] Gerald T. Seidler,[†] Jean-Luc Brédas,[∥] Seth R. Marder,[∥] Jeanne E. Pemberton,*[,‡] and David S. Ginger*[,§]

[†]Department of Physics, University of Washington, Seattle, Washington 98195-1560, United States

[‡]Department of Chemistry and Biochemistry, University of Arizona, Tucson, Arizona 85721, United States

[§]Department of Chemistry, University of Washington, Seattle, Washington 98195-1700, United States

[∥]School of Chemistry and Biochemistry and Center for Organic Photonics and Electronics, Georgia Institute of Technology, Atlanta, Georgia 30332-0400, United States

[⊥]Department of Physics and Astronomy, University of Denver, Denver, Colorado 80208, United States

[#]National Renewable Energy Laboratory, Golden, Colorado 80401, United States

[¶]Stanford Synchrotron Radiation Lightsource, 2575 Sand Hill Road MS69, Menlo Park, California 94025, United States

Supporting Information

ABSTRACT: Self-assembled monolayers (SAMs) of dipolar phosphonic acids can tailor the interface between organic semiconductors and transparent conductive oxides. When used in optoelectronic devices such as organic light emitting diodes and solar cells, these SAMs can increase current density and photovoltaic performance. The molecular ordering and conformation adopted by the SAMs determine properties such as work function and wettability at these critical interfaces. We combine angle-dependent near-edge X-ray absorption fine structure (NEXAFS) spectroscopy and polarization modulation infrared reflection absorption spectroscopy (PM-IRRAS) to determine the molecular orientations of a model phenylphosphonic acid on indium zinc oxide, and correlate the resulting values with density functional theory (DFT). We find that the SAMs are surprisingly well-oriented, with the phenyl ring adopting a well-defined tilt angle of 12−16° from the surface normal. We find quantitative agreement between the two experimental techniques and density functional theory calculations. These results not only provide a detailed picture of the molecular structure of a technologically important class of SAMs, but also resolve a long-standing ambiguity regarding the vibrational-mode assignments for phosphonic acids on oxide surfaces, thus improving the utility of PM-IRRAS for future studies.

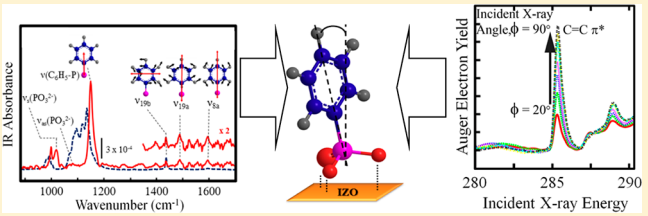

Self-assembled monolayers (SAMs) have been used to improve the performance of electronic devices including organic light-emitting diodes (OLEDs),[1−3] organic field-effect transistors (OFETs),[4] and organic photovoltaics (OPVs).[5,6] SAMs can improve adhesion/wettability of the active layers,[7] control blend phase separation and morphology,[8−10] and are useful for tuning work functions and interfacial barrier heights.[1−3,11,12] Phosphonic acids, in particular, are known to form robust monolayers that increase interfacial compatibility between a transparent conductive oxide and the organic device layer in optoelectronic devices.[7,13,14] While the properties of SAMs such as thiols on coinage metals[14] are well-studied, the molecular level details of technologically relevant SAMs such as aromatic phosphonic acids on transparent conductive oxides are comparatively poorly understood. Data such as the molecular tilt of an aromatic phosphonic acid with respect to the surface are virtually unknown.

Nevertheless, these details are critical to the design and performance of SAM-modified interfaces in thin film electronics. Phosphonic acid binding mode, orientation, and surface coverage can affect the contact angle and work function of modified oxide surfaces.[11,16] The work-function modification can be described as the combination of three effects:[17] (i) the electrostatic potential step (bond dipole) created at the very interface between the oxide surface and the SAM because of the chemical binding; (ii) the possible relaxation of the surface geometry upon binding; and (iii) the electrostatic potential step across the molecular SAM. At the most basic level,[1,10,12,18,19] the magnitude of the latter term, $\Delta\Phi$, is given by

Received: July 24, 2012
Revised: January 19, 2013
Published: January 20, 2013

$$\Delta\Phi = \frac{ne\cdot\mu_{mol}\cos(\theta)}{\varepsilon_0\cdot\varepsilon} \quad (1)$$

Here, μ_{mol} is the molecular dipole moment, θ is the angle the dipole moment makes with the surface normal, ε is the dielectric constant, n is coverage density, e is the charge of an electron, and ε_0 is the vacuum permittivity.[20] However, while quantum-chemical calculations can provide the first two terms, as well as μ_{mol}, the other parameters needed to calculate $\Delta\Phi$, notably n and θ, are best determined experimentally. Even so, with one exception of an insulating alkane phosphonic acid,[21] the tilt angles of most phosphonic acid SAMs have not, to our knowledge, been measured directly.

In this paper, we present a unique and systematic study of the molecular tilt angle of a model phosphonic acid on a transparent conductive oxide that combines both near-edge X-ray absorption fine structure (NEXAFS) spectroscopy and polarization modulation infrared reflection absorption spectroscopy (PM-IRRAS). Cross-correlation of NEXAFS and PM-IRRAS measurements is important for several reasons. Notably, we can both validate the procedures for angle-dependent background subtraction in the NEXAFS data for this class of materials, and we can confirm the IR vibrational mode assignments of the PM-IRRAS data. Comparison to density functional theory (DFT) calculations further strengthens our results.

We chose phenylphosphonic acid (PPA) as our model SAM because it is the simplest representative of a class of SAMs that are known to improve optoelectronic device performance. We selected indium zinc oxide (IZO) for its optical transparency in the infrared region, its ability to form conformal films on a reflective Au substrate (as described below, both attributes are requirements for PM-IRRAS experiments), and its recent utilization in optoelectronic devices.[22,23] We determine the orientation of the phenyl ring using both NEXAFS and PM-IRRAS, and correlate the resulting values with DFT. After correctly assigning the IR vibrational modes observed in PM-IRRAS, we achieve quantitative agreement in the molecular orientation between the two experimental methods, as well as remarkably good agreement with the theoretical predictions.

EXPERIMENTAL SECTION

Both NEXAFS and PM-IRRAS use polarized electromagnetic radiation to extract the orientation of molecular transition dipole moments, but are very different experiments in practice. NEXAFS orientation measurements utilize the directionality of the transition dipole moment associated with soft X-ray excitations of core electrons to molecular antibonding orbitals. Such measurements are well described in the literature,[24−27] and we will only review key details relevant to our experiments and analysis here.

PM-IRRAS orientation measurements probe the orientation of bonds associated with IR excitation of specific molecular vibrational modes. While PM-IRRAS has also been used in similar systems,[5,7,18] ambiguity in earlier vibrational peak assignments requires that we include a discussion of the assignment of vibrational modes, as supported by high-resolution X-ray photoemission spectroscopy (XPS) given in the Supporting Information.

Materials. Evaporated Au on glass slides for PM-IRRAS experiments with 1.5−2.0 nm root-mean-squared (RMS) roughness were purchased from Evaporated Metal Films (Ithaca, NY). PPA was synthesized and purified as described previously.[22] Absolute ethanol was obtained from Aaper Alcohol and Chemical Company (Shelbyville, KY). FTIR-grade KBr was purchased from Alfa Aesar. All chemicals were used as received.

IZO Thin Film Fabrication and Characterization. Au films on glass were selected as the underlying platform for thin IZO films because of their infrared reflectivity. Thin IZO overlayers of 5−10 nm thickness were sputtered onto evaporated Au on glass slides from a 3 in., 70:30 (wt %) In_2O_3:ZnO target in a chamber with a base pressure of 10^{-6} Torr at a deposition pressure of 4.5 mTorr. During an 8.5 s deposition, the oxygen flow was maintained at 0.5 sccm, and the argon flow at 13.4 sccm, with a DC sputtering power of 100 W.

Film continuity (i.e., lack of pinholes) was verified using cyclic voltammetry, and conformity of these sputtered IZO films to the underlying Au-on-glass substrate was further confirmed with atomic force microscopy (AFM). Relevant data are described in the Supporting Information.

Substrate Cleaning and PPA Modification. The thin IZO films produced above were detergent cleaned and sonicated for 10 min in acetonitrile, followed by 5 min in isopropyl alcohol, and dried under an N_2 stream after each step. Next, the substrates were placed into a Harrick Plasma Cleaner PDC-32G (Harrick Plasma, Ithaca, NY) and plasma cleaned for 10 min at an RF power of 10.5 W in a chamber fed by an oxygen pressure of ∼400 mTorr.

Thick film (∼100 nm) IZO on glass substrates was used for NEXAFS data collection and prepared using the same sputtering methods described above. These films were sonicated in acetone for 10 min then scrubbed with Micro-90 electronics-grade detergent in deionized water (DI). Substrates were then successively sonicated in a solution of Micro-90 and DI, then Milli-Q DI, then ethanol, for 10 min each. Substrates were then oxygen plasma cleaned under a 100 mL/min flow of O_2 for 5 min at 18 W power at 100 MHz using a Harrick Plasma PDC-32G plasma cleaner.

All samples were treated with phosphonic acids immediately following plasma cleaning. Samples were immersed in 10 mM phosphonic acid solutions in ethanol for 168 h at room temperature. Upon removal from solution, substrates were rinsed with ethanol, blown dry in a stream of N_2, and annealed under rough vacuum for 2 h at 140 °C. Samples were then rinsed with ethanol and blown dry, then sonicated in a 5% triethylamine/95% ethanol solution (v/v) for 30 min, rinsed well with ethanol, and blown dry. Before IR spectral analysis, the samples were rinsed with ethanol and sonicated for 5 min in ethanol.

NEXAFS. The NEXAFS data were acquired at Stanford Synchrotron Radiation Lightsource (SSRL), at the bending magnet Beamline 8−2.[28] The slit-to-slit SGM monochromator has an optimal resolution of better than 100 meV in the carbon region, but was operated at a lower resolution of about 200 meV for most measurements in order to maximize throughput while still resolving the features needed for the angular dependence analysis. The toroidal refocusing optics provided a near circular beam cross-section of about 1 mm in diameter. The incoming photon flux was recorded from a gold-covered wire mesh (gold grid) intercepting a few percent of the beam, via the drain current by a Keithley picoammeter. In order to ensure a proper normalization without artificial structures from contaminants, a fresh layer of gold was evaporated onto the grid before the start of each run. Second-order contributions from the beamline monochromator were suppressed by a Ti filter, inserted upstream of the gold grid, which strongly absorbs photons above the Ti L-edge at ∼460 eV. The absolute beam energy was calibrated by measuring highly oriented pyrolytic graphite (HOPG), assigning the energy of the π^* feature to 285.38 eV.[29] To compensate for small monochromator drifts over the course of the day, the lower energy dip in the gold-grid absorption spectrum (corresponding the residual carbon on the optics in the beamline and assumed to be constant) was used to align all spectra to the same absolute calibration during individual runs.[28] The degree of linear polarization is assumed to be 0.85±0.05, based on recent measurements on this beamline,[28] although one paper has reported polarization as high as 0.99.[26] The uncertainty in polarization is accounted for in the analysis below, and results in only a 2 degree systematic uncertainty in the final result, with any overestimation of the polarization leading to a measured orientation systematically shifted toward the magic angle, 54.7° (and vice versa).[24] All NEXAFS measurements were conducted at base

dx.doi.org/10.1021/la304594t | Langmuir 2013, 29, 2166−2174

pressures below 10^{-8} Torr. NEXAFS spectra are recorded in two modes simultaneously; total electron yield (TEY), measured as the sample drain current by a Keithley picoammeter, and the Auger electron yield (AEY), measured by a PHI 15−255G double pass cylindrical mirror analyzer (CMA) operated in pulse counting mode. The CMA analyzer was set to a pass energy of 200 eV for highest throughput and operated at a fixed kinetic energy of 257 eV, which is part of the broad carbon Auger distribution and chosen specifically to shift contribution from non-NEXAFS features resulting from first- and second-order photoemission peaks to energies below the onset of the C k-edge NEXAFS spectrum (285 eV). Figure S10 shows a typical AEY spectrum of PPA. Section IV of the Supporting Information discusses subtraction of photoemission features,[24] spectral processing, and uncertainty analysis.

PM-IRRAS. A Nicolet Nexus 670 Fourier transform infrared (FTIR) spectrometer coupled to a tabletop optical module was used to record PM-IRRAS. Polarization modulation (PM) in this instrument was provided by a Hinds Instruments (Hillsboro, OR) PM-90 with a 50 kHz ZnSe optical head and a synchronous sampling demodulator (GWC Instruments, Madison, WI). Detection was accomplished with a MCT-A detector (Thermo Electron Scientific Instrument Corp., Beverly, MA). Samples were positioned to accommodate an 80° angle for incident and reflected radiation; spectra were acquired by averaging 4096 scans at 4 cm^{-1} resolution with spectra acquired in two discrete data sets with maximum dephasing at either 2900 or 1300 cm^{-1} in an effort to minimize PM error across the spectrum.

Reference spectra were acquired (at identical sample placement) on samples that were identically cleaned and placed into neat ethanol for the same soaking period.

Baseline-corrected PM-IRRAS spectra were obtained according to practices previously established in the literature by normalization to the reference spectrum.[30−34] Once corrected for baseline, PM-IRRAS spectra are given by[32,33]

$$\left[\frac{\Delta R}{R}\right]_{\text{norm}} = 1 + \frac{2\gamma\rho}{1-\gamma^2\rho^2}A \qquad (2)$$

where $[\Delta R/R]_{\text{norm}}$ is the baseline-correct PM-IRRAS signal, A is the absorbance, γ is the ratio of overall optoelectronic response for p- and s-polarizations, and ρ is ratio of the reflectivity values of p- and s-polarizations for a reference system of known thickness. For a typical monolayer sample on a metal substrate at grazing angle,[33] γ was determined to be 1 and ρ was determined to be 0.95 at both 2900 and 1000 cm^{-1} on our instrument. Thus, absorbance values were determined from eq 3:[32,33]

$$A = 0.0223\left[\left(\frac{\Delta R}{R}\right)_{\text{norm}} - 1\right] \qquad (3)$$

Band fitting was performed with 100% Gaussian line shapes. Spectral fits were accepted for χ^2 values >0.99.

Transmission spectra of KBr pellets of the neat and dibasic sodium salts of the PAs were acquired on a Nicolet Magna 550 Series II FTIR spectrometer equipped with a MCT-A detector. Acquired spectra were averaged over 512 scans at 4 cm^{-1} resolution.

THEORETICAL CALCULATIONS

Density functional theory calculations were carried out to optimize the adsorption geometry of PPA molecules on a conducting oxide surface. We have evidence suggesting IZO is amorphous (see section I of the Supporting Information), which presents a challenge with respect to our use of slab calculations (see below). Therefore, for the purposes of computation we consider PPA bound to a model indium tin oxide (ITO) surface. We anticipate similar binding geometries on both oxides. This is based on the fact that Sn:In ratio in the commercial ITO is on the order of 0.1−0.2, whereas the Zn:In ratio in our IZO samples is ∼0.24. Therefore, in both cases, the major interaction between the PPA molecules and the substrate is via the surface In atoms, which are common to both ITO and IZO.

The theoretical model of the bare ITO surface consisted of a slab of three (In/Sn−O) layers, where the top layer was passivated by hydroxyl groups.[35] We first consider a low coverage density in order to assess the geometry adopted by a PPA molecule on the surface in the absence of strong interactions among SAM molecules with one phosphonic acid molecule per ITO surface unit cell (24.79 × 14.32 $Å^2$), which is equivalent to 2.8 × 10^{13} molecules/cm^2. In order to evaluate the effect of intermolecular interactions on the variation of the tilt angle, we then consider a higher coverage density of 1.1 × 10^{14} molecules/cm^2, equivalent to four PPA molecules in a unit cell (structure shown in Figure S6 in the Supporting Information). As in our previous work, the Vienna Ab Initio Simulation Package (VASP)[36,37] was used at the GGA-PBE[38] level of theory with the projector-augmented wave (PAW) method.[39] A plane wave cutoff of 300 eV for all elements and a total energy convergence of 10^{-6} eV for the self-consistent iterations were applied in all calculations. The geometry optimizations for the PA-ITO interface systems were performed using a damped molecular dynamics scheme until the forces were 0.04 eV/Å, while the phosphonic acid molecules, the first (In/Sn−O) layer, and all the OH groups on the surface were fully relaxed. All the self-consistent calculations were carried out with the improved tetrahedron method with Blöchl corrections[40] for Brillouin-zone integrations on a 2 × 2 × 1 k-point grid. After optimizing PA/ITO interface geometry, the tilt angle for each phosphonic acid molecule was obtained simply by using the coordinates of their component atoms.

RESULTS AND DISCUSSION

We first consider the molecular orientation as determined by NEXAFS. Figure 1a shows NEXAFS AEY spectra obtained at

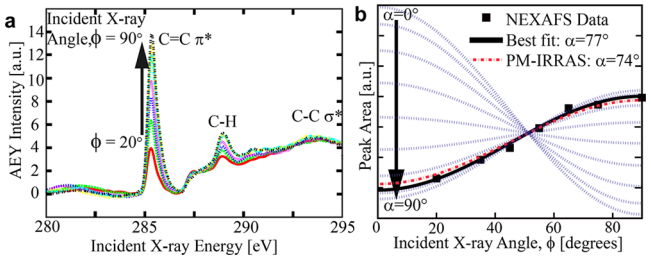

Figure 1. (a) NEXAFS AEY spectra of PPA on IZO at various incident angles from 20° to 90°, the angular dependence of the C=C π^* feature is highlighted. (b) The angular dependence of the peak area under the C=C π^* feature. Superposed are the model fits (eq 2) for α = 0−90° in steps of 10° (dashed blue lines) as well as the best fit of the model to our data (solid black). The red dashed line represents the orientation given by the PM-IRRAS results discussed below. The data shown have been corrected for the angle-dependent IZO background, and processed as described in the experimental methods section.

SSRL for PPA on IZO substrates for different incident X-ray angles, α, from 20° to 90° (normal incidence). We assign the prominent peaks at 285.5 and 288.8 eV to transitions from the C1s to the π^* antibonding orbital of the phenyl ring, and to features of the C−H bonds, respectively. Other notable features include transitions from the 1s to the C−C σ^* antibonding orbitals at 290−310 eV. All assignments are in good agreement with their expected positions.[24] The transition dipole moment

dx.doi.org/10.1021/la304594t | Langmuir 2013, 29, 2166−2174

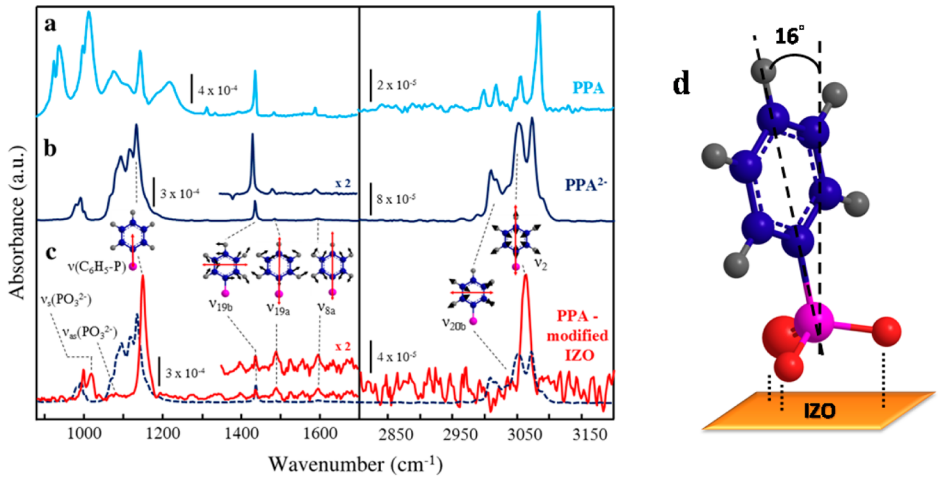

Figure 2. FTIR transmission spectra of (a) PPA (aqua) and (b) PPA^{2-} (dark blue); (c) PM-IRRAS spectrum of PPA-modified IZO (red) and calculated spectrum for 7.4-Å-thick isotropic PPA^{2-} layer (dark blue dashed); and (d) proposed orientation for PPA on IZO from PM-IRRAS.

for the C1s to π^* antibonding orbital of the C═C bonds in an aromatic molecule is normal to the ring structure, and thus provides a convenient peak for determining the orientation of the molecular axis. The strong angular dependence of the C1s to C═C π^* shows that the molecules adopt a preferred orientation relative to the surface. The angle that the transition dipole moment makes with the surface normal, ϕ, can be determined quantitatively by analyzing the NEXAFS peak areas, I_v (ϕ), taken for different incident X-ray angles, α (see eq 4).[24] We assume no preferred direction in the plane of the monolayer and thus average the data over azimuthal orientation.

$$I_v(\phi) \propto \frac{0.85}{3}(1 + 0.5(3\cos^2(\phi) - 1)(3\cos^2(\alpha) - 1)) + \frac{0.15}{2}\sin^2(\alpha) \quad (4)$$

Figure 1b shows the integrated peak area for the C1s to C═C π^* peak at 285.5 eV, along with sample curves showing the expected angular dependence for $\alpha = 0°$ to 90° in 10° steps for reference. The black solid line in Figure 1b is the best fit to the data, yielding an orientation of the phenyl ring normal of $\phi = 77 \pm 5°$ from the surface normal; from geometric considerations, this gives a tilt angle of the phenyl plane of $13 \pm 5°$ from the surface normal, indicating that the phenylphosphonic acid is standing nearly vertically off the IZO surface.

As noted in section IV of the Supporting Information, the uncertainty ±5° is dominated by potential systematic errors associated with uncertainties in the background subtraction and uncertainty in beam polarization. The quoted uncertainty should not be interpreted as the range of angles accessible to a PPA molecule on the IZO surface. Rather, it is the statistical and systematic uncertainty in determining our result, which is a representative value of a distribution of orientations. The width of the distribution of orientations is related to molecule−molecule variation due to surface roughness and, in this case, changes in binding mode. We note however, that while our surfaces are amorphous, they are very smooth as determined by AFM (RMS roughness <0.5 nm) and are below the threshold where roughness effects were shown to emerge in studies of alkane phosphonic acids on indium tin oxide.[21] Nevertheless, these errors are relatively small, and the strong angle dependence of the data, along with the fact that our result is far from the magic angle (~54.7°), is indicative of a well-ordered system.[24] This orientation value is also in excellent agreement with the PM-IRRAS values (see below), further validating both our background subtraction methods, as well as the IR vibrational mode assignments that are discussed in detail in the next section. Though our main goal here is to determine tilt angle, comparison of NEXAFS and density functional theory calculations provide some insight into the nature of PPA−substrate interactions. A calculation performed for a layer of PPA molecules bonded to indium tin oxide at the low packing density of $\sim 2.8 \times 10^{13}$ molecules/cm^2 (as described in the Theoretical Calculations section) suggest the presence of both tridentate and bidentate binding modes (see Figure S8 in the SI). The tridentate configuration is defined with all three oxygen atoms in the PO_3 moiety covalently bonded to metals and exhibits an orientation of 11−12°. The bidentate configuration, defined as two oxygen atoms in the PO_3 moiety covalently bonded to metals and the remaining hydrogen bonded to surface hydroxyls, exhibits an orientation of 15−22°. These values, especially the tridentate, are in excellent agreement with the NEXAFS result above and the PM-IRRAS results that follow. Further discussion of binding mode is provided in section III of the Supporting Information.

Computed at the higher coverage density of $\sim 1.1 \times 10^{14}$ molecules/cm^2, we found that the largest change in the tilt angle for the four PPA molecules is only 6° in comparison with the low coverage case, and the change in the average tilt angle for the four PPA molecules is only 1.5°. The good agreement between the DFT values for both coverages and our measured values indicates that ignoring intermolecular forces in the monolayer provides for a good first approximation in this system.

PM-IRRAS. PM-IRRAS measurements provide a valuable complement to the results from NEXAFS. In order to extract quantitative information about the orientation of surface-bound phosphonic acid molecules using PM-IRRAS, spectral lines arising from vibrational modes with well-defined transition dipole moments must first be identified. This requires selection of an appropriate model system for the surface-confined phosphonic acid as well as a thorough understanding of the vibrational behavior of the surface-confined molecules. Figure 2a,b shows transmission IR spectra of KBr pellets of PPA and

dx.doi.org/10.1021/la304594t | *Langmuir* 2013, 29, 2166−2174

its disodium salt, PPA^{2-}, respectively. Table S1 of the Supporting Information contains the important peak frequencies and their assignments.

The literature contains a thorough discussion of the vibrational spectroscopy of PPA.[18,41−47] However, given that we use the spectrum of PPA^{2-} as a model for the surface form of chemisorbed PPA on IZO surfaces (see below), we explore here the PPA^{2-} spectrum and differences in its spectrum compared to that of PPA. Upon full deprotonation of PPA, significant spectral changes include disappearance of the ν_s(POH) bands at 925 and 939 cm^{-1} and the ν(P−O) band at 1081 cm^{-1} from the $-PO_3H_2$ moiety, coupled with appearance of the $\nu_s(PO_3)$ bands from the PO_3^{2-} moiety between 1015 and 1080 cm^{-1}, and the corresponding $\nu_{as}(PO_3)$ bands appearing as a split multiplet between 1040 and 1160 cm^{-1}.[7,43−45,48] Also, the spectrum for PPA^{2-} does not contain the band at 1220 cm^{-1}, which is present in the PPA spectrum and corresponds to the free ν(P═O) vibration. The ν_{19b}, ν_{19a}, and ν_{8a} phenyl ring modes are present in the spectra for both PPA and PPA^{2-} near 1440, 1490, and 1590 cm^{-1},[49] respectively. The ν_{20b}, ν_2, and ν_{20a} C−H ring modes are also observed near 3020, 3060, and 3080 cm^{-1},[49] respectively, in both spectra.

Figure 2c shows the PM-IRRAS spectrum of IZO modified with a monolayer of PPA. It is noted that this spectrum (solid red line in Figure 2c) is shown on a *y*-axis scale in absorbance units; these absorbance values are obtained by proper conversion of the raw PM-IRRAS data as described in detail in the Experimental Section.[30−34] This spectrum is noticeably simpler than either of the spectra for PPA or PPA^{2-} due to the confluence of PPA orientation on the IZO surface and IRRAS surface selection rules from the underlying Au substrate. In the fingerprint region, only a single intense band centered at ∼1150 cm^{-1} with asymmetry on the high-energy side is observed. In addition, weak bands are also distinguishable at 997, 1017, 1438, 1491, and 1598 cm^{-1}. In the ν(C−H) region around 3000 cm^{-1}, only a single band is observed at 3060 cm^{-1}.

A cursory comparison of the spectra for PPA, PPA^{2-}, and the PPA-modified IZO surface indicates that the bands at 925 and 939 cm^{-1} in the PPA spectrum assigned to ν(P−O−H) modes are absent for PPA on the IZO surface, as the band at 1220 cm^{-1} in the PPA spectrum is assigned to the free ν(P═O) vibration. In the literature, the absence of these bands indicates the oxide surface-confined PPA exists in the PPA^{2-} form with either bidentate or tridentate binding to the oxide surface.[7,18,42,44,45,50]

Further consideration of the spectrum of PPA on the IZO surface reveals that the intense mutiplet of bands between 1060 and 1100 cm^{-1} assigned to $\nu_{as}(PO_3^{2-})$ modes in the PPA^{2-} spectrum is absent from the PM-IRRAS spectrum; we expect this vibration in the vicinity of 1090−1100 cm^{-1} based on the spectral behavior of metal phosphonates.[51,52] The ν_{19b}, ν_{19a}, and ν_{8a} normal phenyl ring modes, near 1440, 1490, and 1590 cm^{-1}, respectively,[49] appear in all three spectra shown in Figure 2, but the ν_{19b} is especially weak and the ν_{19a} is enhanced in the spectrum of surface PPA. The ν_{20b}, ν_2, and ν_{20a} C−H modes are observed near 3020, 3060, and 3080 cm^{-1}, respectively.[49] The ν_{20a} and ν_{20b} bands are also especially weak in the spectrum of surface PPA. We hypothesize these low intensities to be the result of IRRAS surface selection rules and the high degree of order in the PPA monolayer on the IZO surface.

The presence of oriented electric fields at the surface of the IZO/Au substrate allows evaluation of the PM-IRRAS spectral data quantitatively, so that an average tilt angle for the PPA molecules on the IZO surface can be determined. Previous vibrational spectroscopy studies of PPA on a variety of metal oxide substrates have collectively resulted in two conclusions about surface binding and orientation:[18,43,44,53] (1) the spectral signature for oxide-bound PPA is similar to that of PPA^{2-} and the metal phosphonates, and (2) qualitatively, the molecule is oriented in a largely upright position. However, no studies have quantitatively established the average tilt angle of the molecular axis for a phosphonic acid on any metal oxide using PM-IRRAS.

Comparing previous studies and the data reported here, we emphasize the importance of the type of IR spectroscopy used to acquire the spectral data. For example, in several previous studies, simple transmission or diffuse reflectance FTIR spectroscopies were utilized to investigate phosphonic acid layers on oxide particles or powders.[42−44,50] In these studies, all IR-allowed vibrational modes of the phosphonic acid surface species are observed in the surface spectra. In contrast, due to the existence of surface selection rules in IRRAS studies at reflective metal substrates,[7,18] certain IR-allowed vibrational bands may disappear from a spectrum depending on the orientation of the molecule with respect to the surface. We use the observed IRRAS intensities resulting from the operation of these surface selection rules at IZO-covered Au substrates to extract the average molecular tilt angle for monolayers of PPA on IZO.

We now proceed to interpret the IRRAS data in order to determine the average molecular tilt angle. We define the tilt angle as the angular deviation of the molecular axis, the line through the P atom−C1−C4 ring atoms, from the surface normal. In order to determine average molecular orientation within the modifier layer, the experimental IR absorbance spectrum calculated by conversion of the baseline-corrected PM-IRRAS data as described above must be compared to a spectrum that is calculated for an isotropic film of comparable thickness. This is accomplished according to published protocols[54,55] as described in the Supporting Information. The spectrum for an isotropic layer of absorber of a given thickness is calculated using a three-phase model, as reported previously.[54,55] For the PPA monolayer on IZO, we use a thickness of 7.4 Å as determined from X-ray crystallographic data for related metal phosphonates[56−59] and theory.[13] Figure 2c shows the calculated spectrum for an isotropic layer of PPA of this thickness as the dashed line. With the calculated spectrum of an isotropic layer in hand, subsequent data analysis starts from the assumption that the surface-bound PPA exists as the PPA^{2-} form, such that any differences in intensities between the IRRA spectrum and the calculated spectrum for vibrational modes with transition dipole moments along different coordinates indicate a preferred orientation of the surface-bound molecules. From these relative intensity changes, the average orientation of surface-confined molecules is deduced as follows.

For a collection of oriented surface molecules in an external-reflection geometry, there is electric field amplitude at infrared frequencies only normal to the surface. Thus, the integrated absorbance for a vibrational band is proportional to the square of the electric field amplitude at the surface, the magnitude of the transition dipole moment (μ), and the tilt angle θ of μ from the surface normal[60]

$$A \propto (\mu \cdot \cos\theta)^2 \quad (5)$$

dx.doi.org/10.1021/la304594t | Langmuir 2013, 29, 2166−2174

As shown by Hansen[54] and McIntyre,[55] due to this anisotropy of surface electric field amplitude, the integrated absorbance of a mode with a transition moment oriented along the surface normal will be three times as large as the integrated absorbance of the same vibrational band for an isotropic collection of identical molecules in a thin film of equivalent thickness and molecular density. Thus, the tilt angle of a given transition dipole moment can be calculated using

$$\cos\theta = \frac{A_{\mathrm{film}}}{3 \cdot A_{\mathrm{simulated}}} \tag{6}$$

Here, A_{film} is the integrated absorbance of a PPA band from the IZO surface spectrum. In order to properly ratio A_{film} to the value of $A_{\mathrm{simulated}}$, the integrated absorbance of the identical PPA^{2-} band from the calculated spectrum for an isotropic thin film of comparable thickness, both A_{film} and $A_{\mathrm{simulated}}$ must be corrected for molecular density. For A_{film}, this requires a value for surface coverage of PPA on the oxide as well as a monolayer thickness. Here, we use a surface number density of 1.56×10^{14} molecules/cm^2 for monolayer coverage from past experimental studies of alkylphosphonic acids and related systems[7,17,18] and a monolayer thickness of 7.4 Å as determined from X-ray crystallographic data for related metal phenylphosphonates[56−59] and theory.[13] $A_{\mathrm{simulated}}$ is the integrated absorbance of the identical PPA^{2-} band from the calculated spectrum for an isotropic thin film of comparable thickness, corrected for a bulk molecular density of 1.6 g/cm^3.[59]

Quantification of the average tilt angle for PPA molecules on IZO requires identification of appropriate vibrational modes. Suitable spectral bands for this purpose are those which arise from a vibrational mode with a well-defined transition dipole moment, are spectrally well-isolated and clearly identifiable, and are not complicated by splitting. The latter requirement eliminates use of the $\nu_s(PO_3^{2-})$ and $\nu_{as}(PO_3^{2-})$ bands, since they exhibit significant splitting in the spectrum of the model PPA^{2-} and similar metal phosphonates. Spectral bands that meet these requirements are those corresponding to vibrations of the phenyl ring and the C_6H_5−P stretch. The ν_{19b}, ν_{19a}, and ν_{8a} phenyl ring modes near 1440, 1490, and 1590 cm^{-1}, respectively,[49] are excellent choices for tilt angle determination. Each of these vibrations is an in-plane ring vibration with the well-defined transition dipole moments shown on the spectrum in Figure 2c. Moreover, these modes are close in frequency and are spectrally discrete, hence their utility for tilt angle determination.

As noted above, the ν_{19b} mode is especially weak in the surface spectrum for PPA on IZO. This observation immediately suggests that the molecules are oriented such that the transition moment for this mode is largely parallel to the surface. However, given that the transition moment for this mode is orthogonal to the molecular axis, little insight into tilt angle of the molecular axis can be deduced from this conclusion, since PPA could be oriented at a range of tilt angles from 0° to 90° while still maintaining the transition moment of the ν_{19b} mode parallel to the surface. Thus, we exclude this band from further consideration, and proceed to compute the tilt angle here using the ν_{19a} and ν_{8a} phenyl modes along with the $\nu(C_6H_5$−P) mode.

Using the $\nu(C_6H_5$−P) mode for tilt angle quantification relies on its unambiguous assignment in the surface spectrum. The 1150 cm^{-1} band in the surface spectrum can be fit to two bands with maxima at 1149 and 1166 cm^{-1}, but the assignment of these bands has been controversial in the literature. The more intense of the two bands has been previously assigned to either the $\nu(C_6H_5$−P)[18,43,44] or the $\nu(P{=}O)_{\mathrm{associated}}$.[45] Given that the transition dipole moments of these modes are almost orthogonal, both assignments cannot be correct. We proceed here on the assumption (based on recent density functional theory calculations of the vibrational spectroscopy of PPA[46,47]) that the 1140 cm^{-1} band arises from a combination of the $\nu(C_6H_5$−P) and in-plane ring modes, all with transition dipole moments largely parallel to the molecular axis. We validate this assumption by checking the consistency of the results calculated using this vibrational band with those calculated with other bands with similarly oriented transition dipole moments, as well as against the orientations determined by NEXAFS as described above.

To summarize, the three modes that are used for tilt angle determination are the ν_{19a} and ν_{8a} phenyl modes and the $\nu(C_6H_5$−P) mode, all of which have transition moments along the molecular axis. By utilization of integrated areas determined from peak fitting of the PPA surface spectrum and the PPA^{2-} calculated spectrum, and in the case of the $\nu(C_6H_5$−P) band, spectral decomposition of the complex multiplet envelope in the calculated PPA spectrum, eq 5 can be used to determine the tilt angle, θ. Table S2 summarizes the results of orientation analysis from these three spectral bands. Tilt angles of 16°, 16°, and 15° are determined from analysis of the spectral intensities from the $\nu(C_6H_5$−P), ν_{19a}, and ν_{8a} modes, respectively.

From this collective analysis, an average tilt angle of 16 ± 1° is calculated (Figure 2d), which is in excellent agreement with the value of the angle of the ring plane with respect to the surface normal of 13 ± 5° determined from the NEXAFS, as described above, as well as the theoretically calculated value of 11−12° for PPA on ITO for low surface coverage. As with NEXAFS, this uncertainty should not be interpreted as the range of orientations each PPA molecule can adopt relative to the surface. This uncertainty reflects the confidence interval in the average orientation adopted by a PPA molecule on the surface. The width of the distribution is inaccessible to us, and can be affected by surface roughness. We further note that the agreement of the tilt angle calculated using the $\nu(C_6H_5$−P) band at 1149 cm^{-1} serves both to validate our peak assignment and analysis procedures while also resolving discrepancies of this peak assignment in the literature.

CONCLUSIONS

We have determined orientation of a model SAM, phenylphosphonic acid, on a smooth transparent conductive oxide, IZO, using NEXAFS and PM-IRRAS. Surprisingly, these populations have a well-defined orientation, with the phenyl ring plane tilted at an angle of 15 ± 4° from the surface normal, given by the uncertainty-weighted average of the NEXAFS and PM-IRRAS experiments, in quantitative agreement with DFT calculations for PPA on ITO for low surface coverage. The fact that these molecules form well-oriented SAMs may help explain why these molecules have found notable success in surface modification for organic electronics device applications requiring high-quality thin films.

Experimentally, the combination of both NEXAFS and PM-IRRAS was critical to determining the molecular orientation with confidence. We anticipate that the cross-validation of protocols for analyzing phosphonic acids on transparent conductive oxides provided by this study will enable more rapid future studies of these useful compounds with a high

degree of confidence under a range of conditions. Notably, as part of these studies, we were able to correct earlier vibrational peak assignments in the IR spectra of phosphonic acids that are critical to determining molecular orientation via IRRAS.

Finally, we note that the excellent agreement between the experimental and theoretically predicted tilt angles is particularly striking considering that the simulations involved only noninteracting phenylphosphonic acid molecules. This agreement suggests that the phenylphosphonic acid tilt angle is dominated by the substrate/phosphonic acid interaction rather than intermolecular interactions. It will be interesting for future experiments to determine at what point intermolecular interactions begin to alter the orientation of aromatic phosphonic acid SAMs bound to metal oxides.

■ ASSOCIATED CONTENT

Supporting Information

Section 1 includes discussion of IZO thin film fabrication and characterization with AFM and Electrochemical data. Sections 2 and 3 include XPS studies of the PPA-modified IZO surface, details of the PM-IRRAS spectral interpretation, and a discussion of binding geometry. Section 4 includes NEXAFS spectra processing details. This material is available free of charge via the Internet at http://pubs.acs.org

■ AUTHOR INFORMATION

Corresponding Author

*E-mail: pembertn@email.arizona.edu; ginger@chem.washington.edu.

Notes

The authors declare no competing financial interest.

■ ACKNOWLEDGMENTS

NEXAFS measurements were carried out on Beamline 8-2 at Stanford Synchrotron Radiation Lightsource, a national user facility operated by Stanford University on behalf of the U.S. Department of Energy, Office of Basic Energy Sciences. This paper is based on research supported in part by the Center for Interface Science: Solar-Electric Materials (CIS:SEM), an Energy Frontier Research Center funded through the U.S. Department of Energy, Office of Science, Office of Basic Energy Sciences, under Award Number DE-SC0001084 (M.G., L.S., K.M.K., M.C.S., E.L.R., H.L., A.K.S., J.J.B., J.-L.B., S.R.M., J.E.P., D.S.G.), by the National Defense Science and Engineering Graduate Fellowship program and NSF graduate research fellowship DGE-0644493 (A.J.G.), by the Department of Energy, Chemical Sciences Division, under Grant Number. DE-FG02-09ER16106 (G.T.S.), and also by an award from the Department of Energy Office of Science Graduate Fellowship Program (DOE SCGF), made possible in part by the American Recovery and Reinvestment Act of 2009, administered by ORISE-ORAU under contract no. DE-AC05-06OR23100 (K.M.K.). Partial PM-IRRAS expertise (A.M.) and the PM-IRRAS instrumentation for this work were supported by the National Science Foundation through grant award CHE-0848624 (J.E.P.). The computational resources at Georgia Tech are funded in part by the CRIF Program of the NSF under Award Number CHE-0946869.

■ REFERENCES

(1) Sharma, A.; Haldi, A.; Hotchkiss, P. J.; Marder, S. R.; Kippelen, B. Effect of Phosphonic Acid Surface Modifiers on the Work Function of Indium Tin Oxide and on the Charge Injection Barrier into Organic Single-Layer Diodes. *J. Appl. Phys.* **2009**, *105*, 074511−074516.

(2) MacLeod, B. A.; Horwitz, N. E.; Ratcliff, E. L.; Jenkins, J. L.; Armstrong, N. R.; Giordano, A. J.; Hotchkiss, P. J.; Marder, S. R.; Campbell, C. T.; Ginger, D. S. Built-In Potential in Conjugated Polymer Diodes with Changing Anode Work Function: Interfacial States and Deviation from the Schottky−Mott Limit. *J. Phys. Chem. Lett.* **2012**, *3*, 1202−1207.

(3) Knesting, K. M.; Hotchkiss, P. J.; MacLeod, B. A.; Marder, S. R.; Ginger, D. S. Spatially Modulating Interfacial Properties of Transparent Conductive Oxides: Patterning Work Function with Phosphonic Acid Self-Assembled Monolayers. *Adv. Mater.* **2012**, *24*, 642−646.

(4) Miozzo, L.; Yassar, A.; Horowitz, G. Surface Engineering for High Performance Organic Electronic Devices: the Chemical Approach. *J. Mater. Chem.* **2010**, *20*, 2513−2538.

(5) Beaumont, N.; Hancox, I.; Sullivan, P.; Hatton, R. A.; Jones, T. S. Increased Efficiency in Small Molecule Organic Photovoltaic Cells Through Electrode Modification with Self-Assembled Monolayers. *Ener. Environ. Sci.* **2011**, *4*, 1708−1711.

(6) Bulliard, X.; Ihn, S. G.; Yun, S.; Kim, Y.; Choi, D.; Choi, J. Y.; Kim, M.; Sim, M.; Park, J. H.; Choi, W.; Cho, K. Enhanced Performance in Polymer Solar Cells by Surface Energy Control. *Adv. Funct. Mater.* **2010**, *20*, 4381−4387.

(7) Paniagua, S. A.; Hotchkiss, P. J.; Jones, S. C.; Marder, S. R.; Mudalige, A.; Marrikar, F. S.; Pemberton, J. E.; Armstrong, N. R. Phosphonic acid Modification of Indium-Tin Oxide Electrodes: Combined XPS/UPS/Contact Angle Studies. *J. Phys. Chem. C* **2008**, *112*, 7809−7817.

(8) Park, L. Y.; Munro, A. M.; Ginger, D. S. Controlling Film Morphology in Conjugated Polymer: Fullerene Blends with Surface Patterning. *J. Am. Chem. Soc.* **2008**, *130*, 15916−15926.

(9) Wei, J. H.; Coffey, D. C.; Ginger, D. S. Nucleating Pattern Formation in Spin-Coated Polymer Blend Films with Nanoscale Surface Templates. *J. Phys. Chem. B.* **2006**, *110*, 24324−24330.

(10) DeLongchamp, D. M.; Kline, R. J.; Fischer, D. A.; Richter, L. J.; Toney, M. F. Molecular Characterization of Organic Electronic Films. *Adv. Mater.* **2011**, *23*, 319−337.

(11) Hotchkiss, P. J.; Li, H.; Paramonov, P. B.; Paniagua, S. A.; Jones, S. C.; Armstrong, N. R.; Bredas, J.- L.; Marder, S. R. Modification of the Surface Properties of Indium Tin Oxide with Benzylphosphonic Acids: A Joint Experimental and Theoretical Study. *Adv. Mater.* **2009**, *21*, 4496−4501.

(12) Heimel, G.; Romaner, L.; Zojer, E.; Bredas, J.-L. The Interface Energetics of Self-Assembled Monolayers on Metals. *Acc. Chem. Res.* **2008**, *41*, 721−729.

(13) Cecchet, F.; Lis, D.; Guthmuller, J.; Champagne, B.; Fonder, G.; Mekhalif, Z.; Caudano, Y.; Mani, A. A.; Thiry, P. A.; Peremans, A. Theoretical Calculations and Experimental Measurements of the Vibrational Response of p-NTP SAMs: An Orientational Analysis. *J. Phys. Chem. C* **2010**, *114*, 4106−4113.

(14) Hotchkiss, P. J.; Jones, S. C.; Paniagua, S. A.; Sharma, A.; Kippelen, B.; Armstrong, N. R.; Marder, S. R. The Modification of Indium Tin Oxide with Phosphonic Acids: Mechanism of Binding, Tuning of Surface Properties, and Potential for Use in Organic Electronic Applications. *Acc. Chem. Res.* **2012**, *45*, 337−346.

(15) Vericat, C.; Vela, M. E.; Benitez, G.; Carro, P.; Salvarezza, R. C. Self-Assembled Monolayers of Thiols and Dithiols on Gold: New Challenges for a Well-Known System. *Chem. Soc. Rev.* **2010**, *39*, 1805−1834.

(16) Wood, C.; Li, H.; Winget, P.; Brédas, J.-L. Binding Modes of Fluorinated Benzylphosphonic Acids on the Polar ZnO Surface and Impact on Work Function. *J. Phys. Chem. C* **2012**, *116*, 19125−19133.

(17) Li, H.; Paramonov, P.; Bredas, J.-L. Theoretical Study of the Surface Modification of Indium Tin Oxide with Trifluorophenyl Phosphonic Acid Molecules: Impact of Coverage Density and Binding Geometry. *J. Mater. Chem.* **2010**, *20*, 2630−2637.

(18) Koh, S. E.; McDonald, K. D.; Holt, D. H.; Dulcey, C. S.; Chaney, J. A.; Pehrsson, P. E. Phenylphosphonic Acid Functionaliza-

tion of Indium Tin Oxide: Surface Chemistry and Work Functions. *Langmuir* **2006**, *22*, 6249−6255.
(19) Crispin, X.; Geskin, V.; Crispin, A.; Cornil, J.; Lazzaroni, R.; Salaneck, W. R.; Bredas, J.-L. Characterization of the Interface Dipole at Organic/ Metal Interfaces. *J. Am. Chem. Soc.* **2002**, *124*, 8131−8141.
(20) Koch, N. Energy Levels at Interfaces Between Metals and Conjugated Organic Molecules. *J. Phys.: Condens. Matter* **2008**, *20*, 184008−1840019.
(21) Losego, M. D.; Guske, J. T.; Efremenko, A.; Maria, J. P.; Franzen, S. Characterizing the Molecular Order of Phosphonic Acid Self-Assembled Monolayers on Indium Tin Oxide Surfaces. *Langmuir* **2011**, *27*, 11883−11888.
(22) Kang, J. W.; Jeong, W. I.; Kim, J. J.; Kim, H. K.; Kim, D. G.; Lee, G. H. High-Performance Flexible Organic Light-Emitting Diodes Using Amorphous Indium Zinc Oxide Anode. *Electrochem. Solid-State Lett.* **2007**, *10*, J75−J78.
(23) Cheun, H.; Kim, J.; Zhou, Y.; Fang, Y.; Dindar, A.; Shim, J.; Fuentes-Hernandez, C.; Sandhage, K. H.; Kippelen, B. Inverted Polymer Solar Cells with Amorphous Indium Zinc Oxide as the Electron-Collecting Electrode. *Optics Express* **2010**, *18*, A506−A512.
(24) Stöhr, J. *NEXAFS spectroscopy*; Springer-Verlag: Berlin, 1992.
(25) Dubey, M.; Weidner, T.; Gamble, L. J.; Castner, D. G. Structure and Order of Phosphonic Acid-Based Self-Assembled Monolayers on Si(100). *Langmuir* **2010**, *26*, 14747−14754.
(26) Willey, T. M.; Lee, J. R. I.; Fabbri, J. D.; Wang, D.; Nielsen, M. H.; Randel, J. C.; Schreiner, P. R.; Fokin, A. A.; Tkachenko, B. A.; Fokina, N. A.; Dahl, J. E. P.; Carlson, R. M. K.; Terminello, L. J.; Melosh, N. A.; van Buuren, T. Determining Orientational Structure of Diamondoid Thiols Attached to Silver Using Near-Edge X-ray absorption Fine Structure Spectroscopy. *J. Electron Spectrosc.* **2009**, *172*, 69−77.
(27) Vahlberg, C.; Linares, M.; Villaume, S.; Norman, P.; Uvdal, K. Noradrenaline and a Thiol Analogue on Gold Surfaces: An Infrared Reflection-Absorption Spectroscopy, X-ray Photoelectron Spectroscopy, and Near-Edge X-ray Absorption Fine Structure Spectroscopy Study. *J. Phys. Chem. C.* **2011**, *115*, 165−175.
(28) Tirsell, K. G.; Karpenko, V. P. A General-Purpose Sub-Kev X-Ray Facility at the Stanford-Synchrotron-Radiation-Laboratory. *Nucl. Instrum. Methods Phys. Res., Sect. A* **1990**, *291*, 511−517.
(29) Batson, P. E. Carbon-1s Near-Edge-Absorption Fine-Structure in Graphite. *Phys. Rev. B* **1993**, *48*, 2608−2610.
(30) Frey, B. L.; Corn, R. M.; Weibel, S. C. In *Handbook of Vibrational Spectroscopy*, Chalmers, J. M., Griffiths, P. R., Eds.; John Wiley: Chichester, 2001; Vol. *2*, pp 1042−1056.
(31) Barner, B. J.; Green, M. J.; Saez, E. I; Corn, R. M. Polarization Modulation Fourier Transform Infrared Reflectance Measurements of Thin Films and Monolayers at Metal Surfaces Utilizing Real-Time Sampling Electronics. *Anal. Chem.* **1991**, *63*, 55−60.
(32) Buffeteau, T.; Desbat, B.; Turlet, J. M. Polarization Modulation FT-IR Spectroscopy of Surfaces and Ultra-thin Films: Experimental Procedure and Quantitative Analysis. *Appl. Spectrosc.* **1991**, *45*, 380−389.
(33) Bradley, M. S. *A New Approach to Quantitative Spectral Conversion of PM-IRRAS: Theory, Experiments and Performance Comparisons with Conventional IRRAS*; Application Note: 51368; ThermoFisher Scientific; Madison, WI, 2008.
(34) Buffeteau, T.; Desbat, B.; Blaudez, D.; Turlet, J. M. Calibration Procedure to Derive IRRAS Spectra from PM-IRRAS Spectra. *Appl. Spectrosc.* **2000**, *54*, 1646−1650.
(35) Paramonov, P. B.; Paniagua, S. A.; Hotchkiss, P. J.; Jones, S. C.; Armstrong, N. R.; Marder, S. R.; Bredas, J.-L. Theoretical Characterization of the Indium Tin Oxide Surface and of Its Binding Sites for Adsorption of Phosphonic Acid Monolayers. *Chem. Mater.* **2008**, *20*, 5131−5133.
(36) Kresse, G.; Furthmuller, J. Efficiency of Ab-Initio Total Energy Calculations for Metals and Semiconductors Using a Plane-Wave Basis Set. *Comput. Mater. Sci.* **1996**, *6*, 15−50.
(37) Kresse, G.; Furthmuller, J. Efficient Iterative Schemes for Ab Initio Total-Energy Calculations Using a Plane-Wave Basis Set. *Phys. Rev. B* **1996**, *54*, 11169−11186.
(38) Perdew, J. P.; Burke, K.; Ernzerhof, M. Generalized Gradient Approximation Made Simple. *Phys. Rev. Lett.* **1996**, *77*, 3865−3868.
(39) Blöchl, P. E. Projector Augmented-Wave Method. *Phys. Rev. B* **1994**, *50*, 17953−17979.
(40) Blöchl, P. E.; Jepsen, O.; Andersen, O. K. Improved Tetrahedron Method For Brillioun-Zone Integrations. *Phys. Rev. B* **1994**, *49*, 16223−16233.
(41) Daasch, L. W.; Smith, D. C. Infrared Spectra of Phosphorous Compounds. *Anal. Chem.* **1951**, *23*, 853−868.
(42) Randon, J.; Blanc, P.; Paterson, R. Modification of Ceramic Membrane Surfaces Using Phosphoric Acid and Alkyl Phosphonic Acids and its Effects on Ultrafiltration of BSA Protein. *J. Membr. Sci.* **1995**, *98*, 119−129.
(43) Persson, P.; Laiti, E.; Ohman, L. O. Vibration Spectroscopy Study of Phenylphosphonate at the Water-Aluminum (Hydr)Oxide Interface. *J. Colloid Interface Sci.* **1997**, *190*, 341−349.
(44) Guerrero, G.; Mutin, P. H.; Vioux, A. Anchoring of Phosphonate and Phosphinate Coupling Molecules on Titania Particles. *Chem. Mater.* **2001**, *13*, 4367−4373.
(45) Botelho do Rego, A. M.; Ferraria, A. M.; El Beghdadi, J.; Debontridder, F.; Brogueira, P.; Naaman, R.; Rei Vilar, M. Adsorption of Phenylphosphonic Acid on GaAs (100) Surfaces. *Langmuir* **2005**, *21*, 8765−8773.
(46) Forner, W.; Badawi, H. M. Phenylphosphonic and Phenylthiophosphonic Acid and Their Complete Assignment. *Z. Naturforsch.* **2010**, *65b*, 357−366.
(47) Forner, W.; Badawi, H. M. Study of Vibrational Spectra and Their Assignments for Phenylphosphonic Acid and Phenylthiophosphonic Acid and Comparison to Experiments. *J. Struct. Chem.* **2011**, *52*, 471−479.
(48) John, A.; Philip, D.; Cabeza, A.; Devanarayanan, S.; Devanarayanan, S. Vibrational Analysis of Lead(II) Phenylphosphonate Pb(O3PC6H5). *Indian J. Phys.* **2002**, *76B*, 213−215.
(49) Varsanyi, G. *Vibrational Spectra of Benzene Derivatives*; Academic Press: New York, 1969.
(50) Gao, W.; Dickinson, L.; Grozinger, C.; Morin, F. G.; Reven, L. Self-Assembled Monolayers of Alkylphosphonic Acids on Metal Oxides. *Langmuir* **1996**, *12*, 6429−6435.
(51) Seip, C. T.; Granroth, G. E.; Meisel, M. W.; Talham, D. R. Langmuir-Blodgett Films of Known Layered Solids: Preparation and Structural Properties of Octadecylphosphonate Bilayers with Divalent Metals and Characterization of a Magnetic Langmuir-Blodgett Film. *J. Am. Chem. Soc.* **1997**, *119*, 7084−7094.
(52) Fanucci, G. E.; Petruska, M. A.; Meisel, M. W.; Talham, D. R. Structural Characterization and Magnetic Order in Phenoxy-Substituted Divalent Metal Phosphonate Langmuir-Blodgett Films. *J. Solid State Chem.* **1999**, *145*, 443−451.
(53) Ganbold, E.-O.; Lee, Y.; Lee, K.; Kwon, O.; Joo, S.-W. Interfacial Behavior of Benzoic Acid and Phenylphosphonic Acid on Nanocrystalline TiO2 Surfaces. *Chem. Asian J.* **2010**, *5*, 852−858.
(54) Hansen, W. N. Electric Fields Produced by the Propagation of Plane Coherent Electromagnetic Radiation in a Stratified Medium. *J. Opt. Soc. Am.* **1968**, *58*, 380−388.
(55) McIntyre, J. D. E.; Aspnes, D. E. Differential Reflection Spectroscopy of Very Thin Surface Films. *Surf. Sci.* **1971**, *24*, 417−434.
(56) Alberti, G.; Constantino, U.; Allulli, S.; Tomassini, N. Crystalline Zr(R-PO3)2 and Zr(R-OPO3)2 Compounds (R = Organic Radical): A New Class of Materials Having Layered Structure of the Zirconium Phosphate Type. *J. Inorg. Nucl. Chem.* **1978**, *40*, 1113−1117.
(57) Cao, G.; Lee, H.; Lynch, V. M.; Mallouk, T. E. Synthesis and Structural Characterization of a Homologous Series of Divalent Metal Phosphonates, M(II)(O3PR)-H2O and M(II)(HOPR)2. *Inorg. Chem.* **1988**, *27*, 2781−2785.

(58) Martin, K. J.; Squattrito, P. J.; Cleafield, A. The Crystal and Molecular Structure of Zinc Phenylphonsphonate. *Inorg. Chim. Acta* **1989**, *155*, 7−9.
(59) Rao, K. P.; Vidyasagar, K. Syntheses, Structure and Intercalation Properties of Low-Dimensional Phenylphosphonates, A-(HO3PC6H5)(H2O3PC6H5) (A = Alkali metal, NH4, and Tl). *Eur. J. Inorg. Chem.* **2005**, *2005*, 4936−4943.
(60) Allara, D. L.; Nuzzo, R. G. Spontaneously Organized Molecular Assemblies. 2. Quantitative Infrared Spectroscopic Determination of Equilibrium Structures of Solution-Adsorbed n-Alkanoic Acids on an Oxidized Aluminum Surface. *Langmuir* **1985**, *1*, 52−66.